Onsager Reciprocal Relation between Anomalous Transverse Coefficients of an Anisotropic Antiferromagnet

Xiaodong Guo,[1] Xiaokang Li,[1] Zengwei Zhu,[1,*] and Kamran Behnia[2,†]
[1]Wuhan National High Magnetic Field Center and School of Physics, Huazhong University of Science and Technology, Wuhan 430074, China
[2]Laboratoire de Physique et Etude des Matériaux (CNRS/UPMC), Ecole Supérieure de Physique et de Chimie Industrielles, 10 Rue Vauquelin, 75005 Paris, France

(Received 25 July 2023; revised 23 October 2023; accepted 21 November 2023; published 15 December 2023)

Whenever two irreversible processes occur simultaneously, time-reversal symmetry of microscopic dynamics gives rise, on a macroscopic level, to Onsager's reciprocal relations, which impose constraints on the number of independent components of any transport coefficient tensor. Here, we show that in the antiferromagnetic $YbMnBi_2$, which displays a strong temperature-dependent anisotropy, Onsager's reciprocal relations are strictly satisfied for anomalous electric (σ^A_{ij}) and anomalous thermoelectric (α^A_{ij}) conductivity tensors. In contradiction with what was recently reported by Pan *et al.* [Nat. Mater. **21**, 203 (2022)], we find that $\sigma^A_{ij}(H) = \sigma^A_{ji}(-H)$ and $\alpha^A_{ij}(H) = \alpha^A_{ji}(-H)$. This equality holds in the whole temperature window irrespective of the relative weights of the intrinsic or extrinsic mechanisms. The $\alpha^A_{ij}/\sigma^A_{ij}$ ratio is close to k_B/e at room temperature but peaks to an unprecedented magnitude of $2.9k_B/e$ at ~150 K, which may involve nondegenerate carriers of small Fermi surface pockets.

DOI: 10.1103/PhysRevLett.131.246302

Onsager's reciprocal relations are derived by assuming that all microscopic processes are reversible: The future is symmetric to the past [1–7]. This is called time-reversal symmetry. Given a system brought out of equilibrium by the thermodynamic forces F_k, the corresponding fluxes J_i are that, in the coupled transport equation $J_i = \sum_k L_{ik}F_k$, the kinetic coefficients L_{ik} obey the relation $L_{ik} = -L_{ki}$. The time-reversal symmetry is broken when a magnetic field H is applied. This relation states that the kinetic coefficients obey $L_{ik}(H) = L_{ki}(-H)$. This relation, a cornerstone of nonequilibrium statistical physics, is relevant to any case of two irreversible processes occurring simultaneously.

$YbMnBi_2$ crystallizes in a $P4/nmm$ structure, as shown in Fig. 1(a) [8–10]. In an ordered state, the spin of Mn aligns antiferromagnetically along the z axis but with a canted angle that results in a ferromagnetic component in the xy plane [9–12]. This canted ferromagnetic component lifts the degeneracy of Dirac points and creates Weyl points near the Fermi level [9,11]. Both anomalous Hall (AHE) and anomalous Nernst effects were observed in this system [9]. The maximum Nernst thermopower was found to be remarkably large (~6 μVK^{-1} at 160 K), exceeding the Nernst signal observed in other topological antiferromagnets, such as Mn_3Sn [13–15] (~0.5 μVK^{-1}), in Mn_3Ge [14,16,17] (~1.2 μVK^{-1}).

However, Pan *et al.* [9] report an intriguing breakdown of Onsager's reciprocal relations in both Hall and Nernst conductivities. According to their data (Fig. 4 in Ref. [9]), $\sigma_{bc} \neq -\sigma_{cb}$ and $\alpha_{bc} \neq -\alpha_{cb}$ in $YbMnBi_2$, over a wide temperature range. This is surprising, because, in contrast to, say, the Wiedemann-Franz (WF) law, these relations are

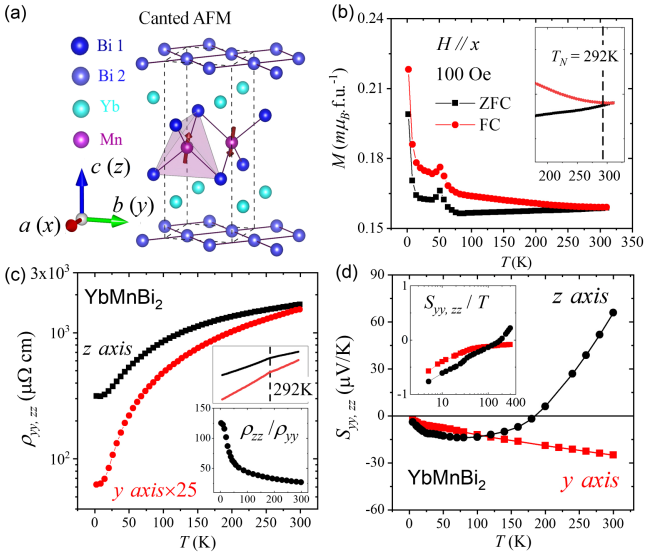

FIG. 1. The basic properties of $YbMnBi_2$. (a) The crystal structure of $YbMnBi_2$ with two sets of Bi: One kind of Bi is bonded to four Mn atoms, while another forms a 2D intercalation network. The spin of Mn cants in the xy plane. (b) Temperature dependence of magnetization M in the xy plane ($H \| xy$). (c) Temperature dependence of longitudinal resistivity ρ_{yy} (red circles) and ρ_{zz} (black squares). (d) Temperature dependence of Seebeck coefficients S_{yy} (red squares) and S_{zz} (black circles).

a cornerstone of irreversible thermodynamics. It has been checked experimentally [18] that, even when the WF law breaks down, the Bridgman relation, a consequence of Onsager reciprocity [5], holds.

The crystal symmetry determines the number of the distinct components of the magnetoconductivity tensors [19,20]. There are cases where components of this tensor (ρ_{ij}, σ_{ij}, or α_{ij},) can have both even (symmetric) and odd (antisymmetric) terms in a magnetic field. The most famous example of this is bismuth and its so-called "umkehr" effect [21,22]. However, the point group crystallographic symmetry of $YbMnBi_2$ rules this out (see Supplemental Note 3 [23]).

Here, we report on a careful study of $YbMnBi_2$ with the aim of quantifying the $zy(cb)$ and $yz(bc)$ components of electric and thermoelectric conductivity tensors. We find that the Hall response obeys Onsager's reciprocal relation. That is, $\rho_{zy}(H) = \rho_{yz}(-H)$ and $\sigma_{zy}(H) = \sigma_{yz}(-H)$. Onsager's reciprocal relations are also verified for the Nernst response: $\alpha_{zy}(H) = \alpha_{yz}(-H)$. On the other hand, and as expected, in the case of Nernst thermopower: $S_{zy}(H) \neq S_{yz}(-H)$. We also examine the temperature dependence of the anomalous transverse thermoelectric response $\alpha^A_{ij}/\sigma^A_{ij}$ ratio [18] and find that this ratio attains a record value of $\approx 2.9 k_B/e$ in this system.

Figure 1(b) shows the temperature dependence of M/H observed under $H = 100$ Oe. The Néel temperature T_N is ~292 K [9,10] revealed by a separation point between the field cooling (FC) and the zero field cooling (ZFC), which agrees with previous reports ~290 K [8,9,11]. At $T \approx 50$ K, we detect, for both orientations of temperature sweep, an anomaly not detected before. It indicates a change in the spin canting orientation below and above this temperature.

As illustrated in Fig. 1(c), resistivity is metallic and anisotropic. Both ρ_{yy} and ρ_{zz} exhibit a small kink near the Néel temperature. The resistivity anisotropy is ≈25 at room temperature and constantly amplifies with cooling, becoming ≈125 at low temperature [see the inset in Fig. 1(c)]. This indicates that not only the Fermi velocity is anisotropic, but also the relative weight of different carriers and/or scattering mechanisms changes with cooling.

The Seebeck coefficient is also anisotropic as shown in Fig. 1(d). S_{yy} is monotonic with temperature. In contrast, S_{zz} is nonmonotonic with a peak around 70 K and a sign change above 180 K. This indicates that S_{zz} has two components with different signs and different variations with temperature. Like many other anisotropic conductors, such as cuprates [27] and ruthenates [28], the Seebeck coefficient, anisotropic at high temperatures, becomes almost isotropic at low temperatures. This is what is expected when the rough magnitude of the (normalized) Fermi energy sets the amplitude of the Seebeck coefficient despite the presence of carriers of both signs [29].

Given the large anisotropy between in-plane (ρ_{yy}) and out-of-plane (ρ_{zz}) resistivity, seen in Fig. 1(c), one may wonder about the fate of Onsager's reciprocal relation in the Hall response. As shown in Fig. 2(a), it holds. The Hall resistivity, when the magnetic field is along the x axis, is identical when it is measured in the $zy(yz)$ configuration. Here, $zy(yz)$ corresponds to a current applied parallel to the $y(z)$ axis and a Hall voltage detected in the $z(y)$ direction.

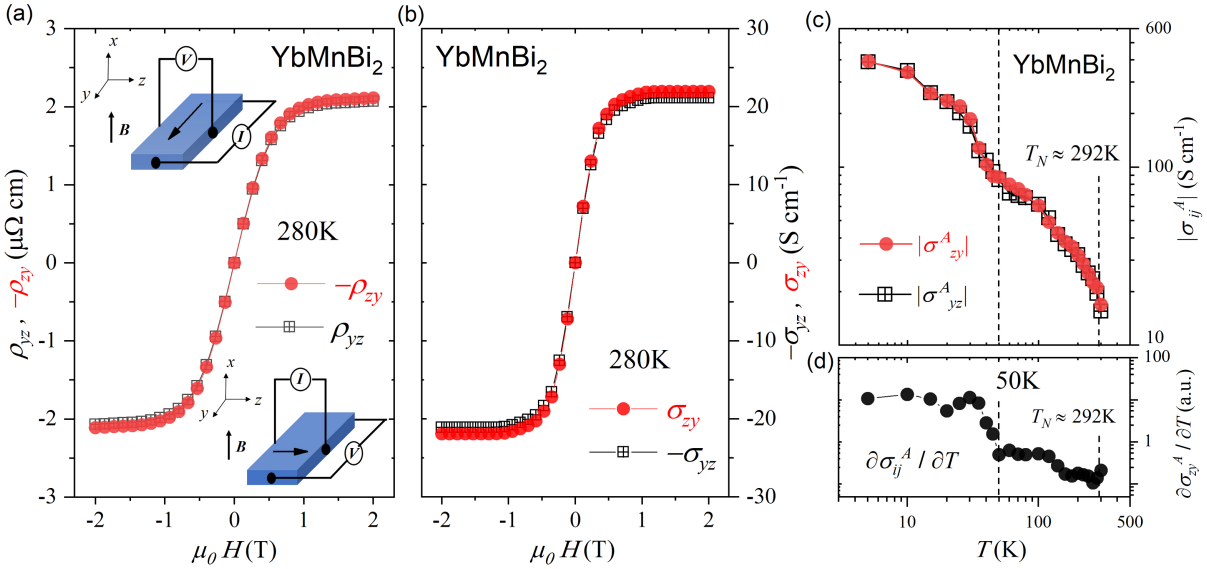

FIG. 2. Transverse electric transport. (a) The setup for measuring Hall signals in the zy and yz configurations. The Hall resistivity is identical: $\rho_{zy} = -\rho_{yz}$. (b) The AHC $\sigma_{zy}(\sigma_{yz})$ at 280 K. The Hall conductivity is also identical: $\sigma_{zy} = -\sigma_{yz}$. (c) The temperature dependence of anomalous Hall conductivity shows that Onsager's reciprocal is true in the whole temperature range. It exhibits turning an anomaly around 50 K, concomitant with an anomaly in magnetization. (d) The temperature derivative of σ^A_{ij}/T, which shows a kink around 50 K.

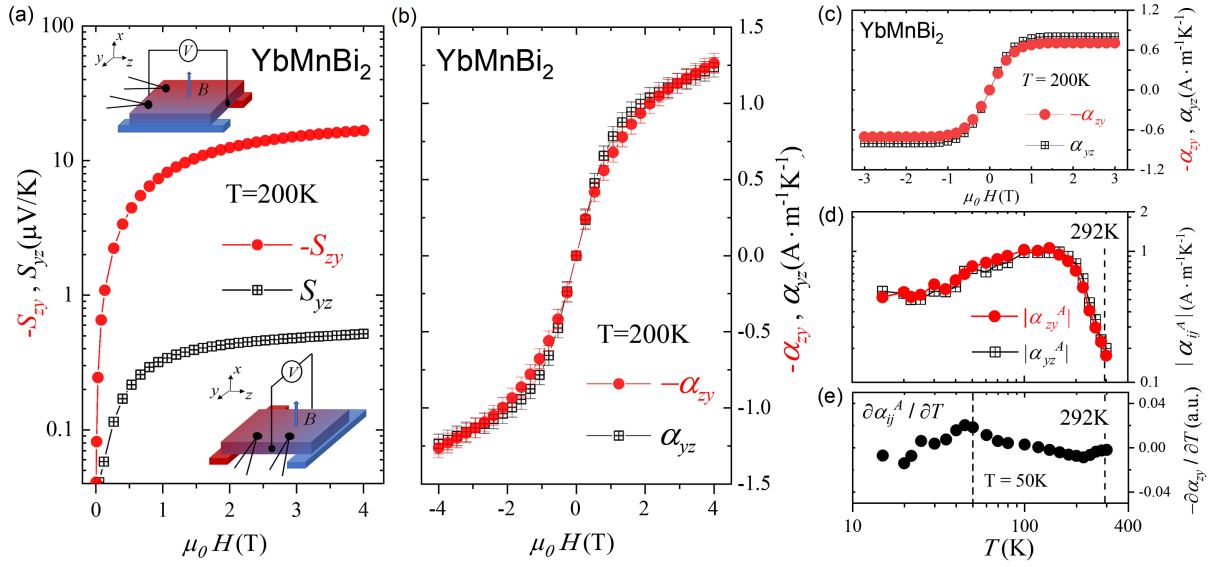

FIG. 3. Transverse thermoelectric transport. (a) The setup for measuring Nernst signals in the zy and yz configurations. The transverse thermopower shows an extreme anisotropy in both reciprocal configurations. (b) The anomalous Nernst conductivity is calculated. Its magnitude for the two configurations is identical within experimental error shown the established Onsager's reciprocal relation. (c) The anomalous Nernst conductivity (ANC) $\alpha_{zy}(\alpha_{yz})$ at 200 K. (d) The temperature dependence of ANC shows that Onsager's reciprocal is true in the whole temperature range. It also exhibits a kink around 50 K. (e) The temperature derivative of α^A_{ij}/T, which shows a kink around 50 K.

Thus, $\rho_{zy}(H) = \rho_{yz}(-H)$. The field sweep reveals a jump representative of the anomalous Hall effect [13,16,30–33]. The Hall conductivity is calculated using $\sigma_{ij} \approx [(-\rho_{ij})/(\rho_{ii}\rho_{jj})]$ in Fig. 2(b). As shown in Fig. 2(c), the two configurations yield identical values for anomalous Hall conductivity (AHC): $\sigma^A_{zy}(H) = \sigma^A_{yz}(-H)$. This equality holds for the whole temperature range [Fig. 2(c)].

Thus, Onsager's reciprocal relation is strictly satisfied for Hall resistivity and Hall conductivity, in the presence of a very anisotropic Fermi surface, a magnetic order, and a temperature-dependent anisotropy. The origin of the observation reported in Ref. [9] is yet to be understood. As discussed in the details in Supplemental Note 5 [23], it might be caused by the oxidation of the samples between two sets of measurements.

Hall conductivities exhibit anomalies around 50 K [Fig. 2(c)], consistent with the anomaly seen in the magnetization data shown in Fig. 1(b). To further illustrate this point, we took the derivative of σ^A_{ij}, as depicted in Fig. 2(d), and identified a distinct anomaly occurring at 50 K. The longitudinal transport does not show any anomaly at 50 K [Fig. 1(c)]. Therefore, what happens at this temperature concerns the orientation of spins. The Fermi surface or other electronic charge-related properties are not visibly affected.

Let us now examine the relevance of Onsager's reciprocity to the thermoelectric transport. In contrast to its electric counterpart, the anomalous Nernst effect is driven by a statistical force [34,35], and the issue deserves to be addressed by the experiment. In Fig. 3(a), we show the results of Nernst experiment for two configurations. In the absence of charge current, when a temperature gradient ∇T, is applied, along the y (z) axis, it gives rise to a voltage along the z (y) orientation. Thus, one can compare the responses for zy and yz configurations. As shown in Fig. 3(a), $S_{zy} \neq -S_{yz}$. At 1 T, the anisotropy is as large as 24. Since S_{ij} is *not* a true Onsager coefficient, this is not a surprising result. On the other hand, α, the thermoelectric conductivity tensor, is an Onsager coefficient which links a force (either the temperature gradient or the electric field) to a flux (the charge density current or the heat density current). The Nernst conductivity is the off-diagonal component of this Onsager tensor: $\alpha_{ij} = S_{ij}\sigma_{ii} + S_{jj}\sigma_{ij}$. It is shown in Fig. 3(b). One can see that $\alpha_{zy} = -\alpha_{yz}$ and they both show a jump during the field sweep near zero magnetic field as observed in numerous magnets [9,13,16,18,36–38], shown in Fig. 3(c). Its magnitude for the two configurations is identical within experimental uncertainty: $\alpha^A_{zy}(H) = \alpha^A_{yz}(-H)$. We found that this equality holds for the whole temperature range [Fig. 3(d)].

Onsager's reciprocal relations lead to the following (details in Supplemental Note 6 [23]):

$$\frac{S_{ij}}{S_{ji}} \approx -\frac{\sigma_{jj}}{\sigma_{ii}}. \tag{1}$$

As in the case of the anomalous Hall effect, there is a kink in S^A_{ij} and α^A_{ij} [Fig. 3(d) and Supplemental Note 6 [23]], near the temperature at which there is an anomaly in magnetization. A more visible anomaly can be seen in the

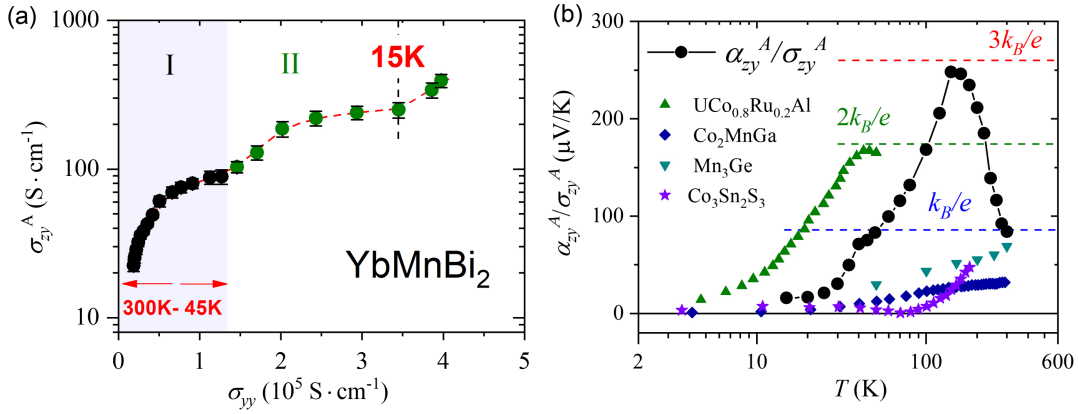

FIG. 4. Scaling relation of the anomalous Hall conductivity. The longitudinal conductivity (a) σ_{yy} for $YbMnBi_2$ lines within the good-metal regime, and there is a crossover behavior to the skew scattering region in the lower temperature, suggesting the skew scattering will dominate the transverse transport. The flat AHC [$\sigma_H^A = (\sigma)^0 = \text{const}$] is concomitant with the maximum of magnetization at 50 K in region I. A second observed intrinsic AHC can be attributed to the magnetization turning point at 15 K in region II. An extrinsic mechanism may play a role by below 15 K. (b) The $\alpha_{zy}^A/\sigma_{zy}^A$ ratio at different temperatures. Similar to other topological magnets, it approaches 86 μV/K at room temperature, but there is a peak as large as 250 μV/K at 150 K.

temperature derivative of α_{ij}^A as presented in Fig. 3(e). The Seebeck coefficient does not show any anomaly at 50 K [Fig. 1(d)]. This further suggests that what occurs at 50 K is a spin-related and not a charge-related phenomenon.

Since Onsager's reciprocity is found to hold in the whole temperature range, let us demonstrate that this implies its validity irrespective of the origin of the anomalous transverse coefficients. Figure 4(a) shows how the amplitude of the anomalous Hall conductivity for the yz configuration varies as a function of longitudinal conductivity as the sample is cooled. Two regions, I and II, can be distinguished in this plot. In region I, at high temperature above the anomaly in magnetization, σ_{zy}^A increases with increasing σ_{yy} and then saturates to a plateau near 50 K. This flat AHC [$\sigma_H^A = (\sigma)^0 = \text{const}$] is concomitant with the maximum of magnetization at 50 K and may be attributed to an intrinsic AHC [18,30,31,39–41]. With decreasing temperature and entrance to region II, magnetization increases to a turning point at 15 K, and the AHC also saturates near the same temperature, representing a second intrinsic AHC. A transformation of the intrinsic Berry curvature at 50 K would explain the observation of two saturated AHC amplitudes around 50 and 15 K. Below 15 K, σ_{zy}^A increases again as a function of σ_{yy}, indicating a role played by an extrinsic (skew scattering or side jump) mechanism of AHE [30,41,42]. The change in the in-plane ferromagnetic component at 50 K affects the intrinsic Berry curvature. Density functional theory (DFT) [43] finds that the number of the Weyl node pairs will increase with increasing canted angle.

Given the presence of both intrinsic and extrinsic components in AHE and the equality between off-diagonal components of AHC and ANC in the whole temperature range, we can conclude that Onsager's reciprocity is relevant to anomalous transverse response regardless of the details of their microscopic origin.

Let us now turn our attention to the relative amplitude of σ_{ij}^A and α_{ij}^A. Xu *et al.* [18] found that the ratio of $\alpha_{ij}^A/\sigma_{ij}^A$ approaches the ratio of natural units $k_B/e = 86\ \mu\text{VK}^{-1}$ at room temperature in many topological magnets. The temperature dependence of the $\alpha_{ij}^A/\sigma_{ij}^A$ ratio is a monotonic function of the temperature and approaches k_B/e near the ordering temperature [24,39,40,44]. In contrast, as shown in Fig. 4(b), we find that, in $YbMnBi_2$, the temperature dependence of this ratio is nonmonotonic and attains a value as large as $2.9k_B/e$ at 160 K.

In the intrinsic picture, this ratio depends on the way the Berry curvature affects the flow of entropy and the flow of charge [18,24]. Roughly, the ratio is set by $[(k_B)/e](\langle\lambda_F^2\rangle/\langle\Lambda^2\rangle)$ [18], where $\langle\lambda_F^2\rangle$ and $\langle\Lambda^2\rangle$ are the square of the Fermi and the thermal wavelengths averaged over the whole Fermi surface, respectively [18]. As the system is warmed up, the $\alpha_{ij}^A/\sigma_{ij}^A$ ratio monotonically increases and tends toward $\sim(k_B/e)$ when λ_F and Λ become comparable. A number of theoretical studies have examined the amplitude of this ratio [25,45]. Qiang *et al.* [25], by performing a Sommerfeld expansion, found that this ratio becomes $(\alpha_{ij}^{\text{int}}/\sigma_{ij}^{\text{int}}) = \{[(\mu/e) + (\pi^2/3)[(k_B^2T^2)/(e\mu)]\}^{-1}L_0T$. This expression implies an upper boundary of $\sim 0.77(k_B/e)$ [25,26] (see Supplemental Note 7 [23]). Therefore, our observation calls for an approach beyond a single-band degenerate Fermi system subject to Sommerfeld expansion.

The Fermi surface of $YbMnBi_2$ is known to consist of multiple electron and hole pockets. According to the most recent set of DFT calculations [9], the largest pockets are electronlike and have a Fermi energy in the range of ~80 meV [8,9,11]. This is confirmed by our Shubnikov-de Haas oscillations (SdH) results (see Supplemental Note 8

[23]) and consistent with the slope of our isotropic thermopower at low temperatures shown in Fig. 1(d). $S_{ii}/T \rightarrow 0.6\ \mu V/K^2$ implies a Fermi energy of ∼50 meV. Since this is the largest energy scale of the system, the Fermi energy of other pockets (and, in particular, the smaller hole pockets) should be significantly smaller than this, and, at 150 K, at least one set of hole pockets are nondegenerate.

There is no available theory of intrinsic anomalous Hall effect in the presence of nondegenerate electrons. Nevertheless, let us note that a nondegenerate electron has more entropy than a degenerate electron [46] but the same electric charge. Therefore, it is plausible that the presence of nondegenerate carriers allows a larger $\alpha_{ij}^A/\sigma_{ij}^A$ ratio. Let us also not forget that the k_B/e boundary may not hold in the presence of multiple bands or when AHE is partially extrinsic.

In summary, we measured electric and thermoelectric transport properties in $YbMnBi_2$ and found that Onsager's reciprocal relation is robust. Reciprocity holds in the whole temperature range irrespective of the intrinsic or extrinsic origin of the anomalous transverse response. The $\alpha_{ij}^A/\sigma_{ij}^A$ ratio is exceptionally large, possibly as a result of the presence of nondegenerate electrons.

This work was supported by The National Key Research and Development Program of China (Grant No. 2022YFA1403500), the National Science Foundation of China (Grants No. 12004123, No. 51861135104, and No. 11574097), and the Fundamental Research Funds for the Central Universities (Grant No. 2019kfyXMBZ071). K. B. was supported by the Agence Nationale de la Recherche (ANR-19-CE30-0014-04). X. L. acknowledges the China National Postdoctoral Program for Innovative Talents (Grant No. BX20200143) and the China Postdoctoral Science Foundation (Grant No. 2020M682386).

*zengwei.zhu@hust.edu.cn
†kamran.behnia@espci.fr

[1] L. Onsager, Reciprocal relations in irreversible processes. I., Phys. Rev. **37**, 405 (1931).
[2] L. Onsager, Reciprocal relations in irreversible processes. II., Phys. Rev. **38**, 2265 (1931).
[3] P. Mazur and S. R. de Groot, Extension of Onsager's theory of reciprocal relations. II, Phys. Rev. **94**, 224 (1954).
[4] S. R. de Groot and P. Mazur, Extension of Onsager's theory of reciprocal relations. I, Phys. Rev. **94**, 218 (1954).
[5] H. B. Callen, The application of Onsager's reciprocal relations to thermoelectric, thermomagnetic, and galvanomagnetic effects, Phys. Rev. **73**, 1349 (1948).
[6] H. B. G. Casimir, On Onsager's principle of microscopic reversibility, Rev. Mod. Phys. **17**, 343 (1945).
[7] K. Behnia, *Fundamentals of Thermoelectricity* (Oxford University Press, New York, 2015).
[8] A. Wang, I. Zaliznyak, W. Ren, L. Wu, D. Graf, V. O. Garlea, J. B. Warren, E. Bozin, Y. Zhu, and C. Petrovic, Magnetotransport study of Dirac fermions in $YbMnBi_2$ antiferromagnet, Phys. Rev. B **94**, 165161 (2016).
[9] Y. Pan, C. Le, B. He, S. J. Watzman, M. Yao, J. Gooth, J. P. Heremans, Y. Sun, and C. Felser, Giant anomalous Nernst signal in the antiferromagnet $YbMnBi_2$, Nat. Mater. **21**, 203 (2022).
[10] J.-R. Soh, H. Jacobsen, B. Ouladdiaf, A. Ivanov, A. Piovano, T. Tejsner, Z. Feng, H. Wang, H. Su, Y. Guo, Y. Shi, and A. T. Boothroyd, Magnetic structure and excitations of the topological semimetal $YbMnBi_2$, Phys. Rev. B **100**, 144431 (2019).
[11] S. Borisenko, D. Evtushinsky, Q. Gibson, A. Yaresko, K. Koepernik, T. Kim, M. Ali, J. van den Brink, M. Hoesch, A. Fedorov, E. Haubold, Y. Kushnirenko, I. Soldatov, R. Schäfer, and R. J. Cava, Time-reversal symmetry breaking type-II Weyl state in $YbMnBi_2$, Nat. Commun. **10**, 3424 (2019).
[12] C. Le, C. Felser, and Y. Sun, Design strong anomalous Hall effect via spin canting in antiferromagnetic nodal line materials, Phys. Rev. B **104**, 125145 (2021).
[13] X. Li, L. Xu, L. Ding, J. Wang, M. Shen, X. Lu, Z. Zhu, and K. Behnia, Anomalous Nernst and Righi-Leduc effects in Mn_3Sn: Berry curvature and entropy flow, Phys. Rev. Lett. **119**, 056601 (2017).
[14] T. Chen, T. Tomita, S. Minami, M. Fu, T. Koretsune, M. Kitatani, I. Muhammad, D. Nishio-Hamane, R. Ishii, F. Ishii, R. Arita, and S. Nakatsuji, Anomalous transport due to Weyl fermions in the chiral antiferromagnets Mn_3X, X = Sn, Ge, Nat. Commun. **12**, 572 (2021).
[15] M. Ikhlas, T. Tomita, T. Koretsune, M.-T. Suzuki, D. Nishio-Hamane, R. Arita, Y. Otani, and S. Nakatsuji, Large anomalous Nernst effect at room temperature in a chiral antiferromagnet, Nat. Phys. **13**, 1085 (2017).
[16] L. Xu, X. Li, X. Lu, C. Collignon, H. Fu, J. Koo, B. Fauqué, B. Yan, Z. Zhu, and K. Behnia, Finite-temperature violation of the anomalous transverse Wiedemann-Franz law, Sci. Adv. **6**, eaaz3522 (2020).
[17] C. Wuttke, F. Caglieris, S. Sykora, F. Scaravaggi, A. U. B. Wolter, K. Manna, V. Süss, C. Shekhar, C. Felser, B. Büchner, and C. Hess, Berry curvature unravelled by the anomalous Nernst effect in Mn_3Ge, Phys. Rev. B **100**, 085111 (2019).
[18] L. Xu, X. Li, L. Ding, T. Chen, A. Sakai, B. Fauqué, S. Nakatsuji, Z. Zhu, and K. Behnia, Anomalous transverse response of Co_2MnGa and universality of the room-temperature $\alpha_{ij}^A/\sigma_{ij}^A$ ratio across topological magnets, Phys. Rev. B **101**, 180404(R) (2020).
[19] Y. Akgoz and G. Saunders, Space-time symmetry restrictions on the form of transport tensors. I. Galvanomagnetic effects, J. Phys. C **8**, 1387 (1975).
[20] Y. Akgoz and G. Saunders, Space-time symmetry restrictions on the form of transport tensors. II. Thermomagnetic effects, J. Phys. C **8**, 2962 (1975).
[21] J. Michenaud, J. Streydio, J. Issi, and A. Luyckx, 'Umkehreffekt' and crystal symmetry of bismuth, Solid State Commun. **8**, 455 (1970).
[22] F. Spathelf, B. Fauqué, and K. Behnia, Magneto-Seebeck effect in bismuth, Phys. Rev. B **105**, 235116 (2022).
[23] See Supplemental Material at http://link.aps.org/supplemental/10.1103/PhysRevLett.131.246302 for more

detailed experimental methods, the form of transverse electrical and thermoelectric transport tensors, the sensitive sample oxidation dependence for the anomalous Hall effect, and the derivations of Nernst thermopower apportioned by the mobility and the derivations of an upper boundary for $\alpha_{ij}^{A}/\sigma_{ij}^{A}$, which includes Refs. [9,10,13,16,18–20,24–26].

[24] L. Ding, J. Koo, L. Xu, X. Li, X. Lu, L. Zhao, Q. Wang, Q. Yin, H. Lei, B. Yan, Z. Zhu, and K. Behnia, Intrinsic anomalous Nernst effect amplified by disorder in a half-metallic semimetal, Phys. Rev. X **9**, 041061 (2019).

[25] X.-B. Qiang, Z. Z. Du, H.-Z. Lu, and X. C. Xie, Topological and disorder corrections to the transverse Wiedemann-Franz law and Mott relation in kagome magnets and Dirac materials, Phys. Rev. B **107**, L161302 (2023).

[26] N. Ashcroft and N. Mermin, *Solid State Physics* (Cengage Learning, Boston, 2011).

[27] T. W. Silk, I. Terasaki, T. Fujii, and A. J. Schofield, Out-of-plane thermopower of strongly correlated layered systems: An application to $Bi_2(Sr,La)_2CaCu_2O_{8+\delta}$, Phys. Rev. B **79**, 134527 (2009).

[28] R. Daou, S. Hébert, G. Grissonnanche, E. Hassinger, L. Taillefer, H. Taniguchi, Y. Maeno, A. S. Gibbs, and A. P. Mackenzie, Anisotropic seebeck coefficient of Sr_2RuO_4 in the incoherent regime, Phys. Rev. B **108**, L121106 (2023).

[29] K. Behnia, D. Jaccard, and J. Flouquet, On the thermoelectricity of correlated electrons in the zero-temperature limit, J. Phys. Condens. Matter **16**, 5187 (2004).

[30] N. Nagaosa, J. Sinova, S. Onoda, A. H. MacDonald, and N. P. Ong, Anomalous Hall effect, Rev. Mod. Phys. **82**, 1539 (2010).

[31] A. Sakai, Y. P. Mizuta, A. A. Nugroho, R. Sihombing, T. Koretsune, M.-T. Suzuki, N. Takemori, R. Ishii, D. Nishio-Hamane, R. Arita, P. Goswami, and S. Nakatsuji, Giant anomalous Nernst effect and quantum-critical scaling in a ferromagnetic semimetal, Nat. Phys. **14**, 1119 (2018).

[32] S. Nakatsuji, N. Kiyohara, and T. Higo, Large anomalous Hall effect in a non-collinear antiferromagnet at room temperature, Nature (London) **527**, 212 (2015).

[33] Y. Taguchi, Y. Oohara, H. Yoshizawa, N. Nagaosa, and Y. Tokura, Spin chirality, berry phase, and anomalous Hall effect in a frustrated ferromagnet, Science **291**, 2573 (2001).

[34] D. Xiao, Y. Yao, Z. Fang, and Q. Niu, Berry-phase effect in anomalous thermoelectric transport, Phys. Rev. Lett. **97**, 026603 (2006).

[35] D. Xiao, M.-C. Chang, and Q. Niu, Berry phase effects on electronic properties, Rev. Mod. Phys. **82**, 1959 (2010).

[36] N. Hanasaki, K. Sano, Y. Onose, T. Ohtsuka, S. Iguchi, I. Kézsmárki, S. Miyasaka, S. Onoda, N. Nagaosa, and Y. Tokura, Anomalous Nernst effects in pyrochlore molybdates with spin chirality, Phys. Rev. Lett. **100**, 106601 (2008).

[37] T. Miyasato, N. Abe, T. Fujii, A. Asamitsu, S. Onoda, Y. Onose, N. Nagaosa, and Y. Tokura, Crossover behavior of the anomalous Hall effect and anomalous Nernst effect in itinerant ferromagnets, Phys. Rev. Lett. **99**, 086602 (2007).

[38] Y. Pu, D. Chiba, F. Matsukura, H. Ohno, and J. Shi, Mott relation for anomalous Hall and Nernst effects in $Ga_{1-x}Mn_xAs$ ferromagnetic semiconductors, Phys. Rev. Lett. **101**, 117208 (2008).

[39] S. N. Guin, K. Manna, J. Noky, S. J. Watzman, C. Fu, N. Kumar, W. Schnelle, C. Shekhar, Y. Sun, J. Gooth, and C. Felser, Anomalous Nernst effect beyond the magnetization scaling relation in the ferromagnetic Heusler compound Co_2MnGa, NPG Asia Mater. **11**, 16 (2019).

[40] X. Xu, J.-X. Yin, W. Ma, H.-J. Tien, X.-B. Qiang, P. V. S. Reddy, H. Zhou, J. Shen, H.-Z. Lu, T.-R. Chang, Z. Qu, and S. Jia, Topological charge-entropy scaling in kagome Chern magnet $TbMn_6Sn_6$, Nat. Commun. **13**, 1197 (2022).

[41] S. Onoda, N. Sugimoto, and N. Nagaosa, Intrinsic versus extrinsic anomalous Hall effect in ferromagnets, Phys. Rev. Lett. **97**, 126602 (2006).

[42] Y. Tian, L. Ye, and X. Jin, Proper scaling of the anomalous Hall effect, Phys. Rev. Lett. **103**, 087206 (2009).

[43] X.-S. Ni, C.-Q. Chen, D.-X. Yao, and Y. Hou, Origin of the type-II Weyl state in topological antiferromagnetic $YbMnBi_2$, Phys. Rev. B **105**, 134406 (2022).

[44] H. Zhang, J. Koo, C. Xu, M. Sretenovic, B. Yan, and X. Ke, Exchange-biased topological transverse thermoelectric effects in a kagome ferrimagnet, Nat. Commun. **13**, 1091 (2022).

[45] Z. Wang, R. Boyack, and K. Levin, Heat-bath approach to anomalous thermal transport: Effects of inelastic scattering, Phys. Rev. B **105**, 134302 (2022).

[46] C. Collignon, P. Bourges, B. Fauqué, and K. Behnia, Heavy nondegenerate electrons in doped strontium titanate, Phys. Rev. X **10**, 031025 (2020).